Hindawi
Applied and Environmental Soil Science
Volume 2022, Article ID 9118461, 15 pages
https://doi.org/10.1155/2022/9118461

Research Article

Soil Physical Characteristics and Saturated Hydraulic Conductivity in the Landform of Barito Delta, Kalimantan, Indonesia

Deasy Arisanty,[1] **Novi Rahmawati**,[2] **and Dedi Rosadi**[3]

[1]*Department of Geography Education, Faculty of Teacher Training and Education, Lambung Mangkurat University, Brigjen H. Hasan Basry Street, 70123 Banjarmasin, Kalimantan, Indonesia*
[2]*Department of Water Resources, Faculty of Geo-Information Science and Earth Observation (ITC), University of Twente, Enschede, Netherlands*
[3]*Department of Mathematics, Faculty of Mathematics and Natural Sciences, Gadjah Mada University, Sekip Utara, 55281 Yogyakarta, Indonesia*

Correspondence should be addressed to Deasy Arisanty; deasyarisanty@ulm.ac.id

Received 12 January 2022; Revised 7 April 2022; Accepted 19 April 2022; Published 17 May 2022

Academic Editor: Evgeny Abakumov

We explore the soil physical characteristics in wetland of Barito Delta from primary data of soil sample and electrical resistivity measurement with the support from some secondary data. We also estimate saturated hydraulic conductivity (K_s) in Barito Delta from soil physical characteristics applying Saxton and Rawls (1986) and Weynants et al. (2009). Soil texture profile is determined from interpolation of soil fraction in each layer applying Bayesian statistics to analyze soil physical characteristics in the landforms of Delta. Clay is the dominant soil fraction in the soil of Barito Delta. Clay fraction percentage decrease along the depth of soil profile as it reaches fine sand particles deriving from ancient sedimentation from the past. It is an opposite with soil organic matter content that has contrast value from 1st to 2nd soil depth, but a few discrepancy from 3rd depth to downward direction. The content of clay in the soil depends on the sedimentation activity in the landform. Clay is dominant soil particle in the Delta; in case, it is in flat area and there is no intensive of sea water sedimentation such as in Basin of Peat Anticline and Natural Levee. In more than 2 m depth of soil, loamy sand and silty clay textures are mostly in the landform that is influenced by sea water activity, while by river water is clay loam. K_s values from Saxton and Rawls (1986) are close to K_s values from the measurement of previous studies. K_s values are generally small in Barito Delta that is mostly ranging from 1.10^{-7} to $2\ \mathrm{m\ s^{-1}}$. K_s values are larger following the depth of soil profile. The values of K_s are smaller in Basin of Peat Anticline and Natural Levee than in Tidal Flat and Beach Ridge. It is because both landforms have clay as dominant soil particles.

1. Introduction

Physical and hydraulic properties of soil are valuable information for water balance studies and simulations [1]. Physical properties of soil or soil physical characteristics, that is, soil texture, bulk density, and soil organic matter, are used to determine management in agricultural and environmental applications [2]. Soil texture is one of essential factors influencing hydraulic parameter of soils [3] and also can be used as indication to analyze the potential source of water to downgradient ecosystems and water bodies in landforms [4]. The percentage of particle size of sand, silt, and clay in soil material is soil texture. Soil texture classification is useful to determine the soil particle distribution [5, 6] that is essential to estimate soil water hydraulic characteristics [7]. Bulk density is physical properties of soil that varies with soil structure condition. Bulk density is essential for soil compaction information and modern farming technique planning. Organic matter is soil physical characteristics that include all the elements of organic compounds (hydrogen, oxygen, nitrogen, etc.). It is important information for plants nutrients [8].

It has been long term applied that soil physical characteristics are used for soil water hydraulic characteristics [9]. One of dominant soil hydraulic characteristics is saturated hydraulic conductivity [5]. Estimation of saturated hydraulic conductivity (K_s) is important because it is the main key of soil characteristics [10]. It describes the rate of water flow and one of the parameters to predict soil hydraulic behavior. It represents the ability of soil to transmit the water in saturated zone [11]. It is also the key to evaluate soil water movement and quality [10]. K_s is also important to understand soil moisture dynamics [12], resources management decision related to water conservation [11], and plant growth [5, 11].

Soil water characteristics are used to estimate K_s from soil physical characteristics [9]. Soil physical characteristics that are commonly used to estimate saturated hydraulic conductivity are particle size distribution, bulk density, and organic matter compound [13]. Soil texture and bulk density are mostly easy to obtain to estimate K_s [11, 14]. Bulk density and soil texture are commonly soil physical properties that are used to estimate K_s using pedotransfer function [15, 16]. Pedotransfer function of K_s also can be predicted from organic matter compound [17]. Pedotransfer functions (PTFs) are developed from soil properties by linking soil survey maps with representative soil profiles [18]. K_s can be determined from soil profiles from each soil depth applying this technique. Soil hydraulic properties with respect to horizons are required to obtain information of overall hydraulic behavior of soil profile [19] in each depth.

PTFs are important to quantify and to predict ecosystem services of soil such as for food supply and water storage. Land surface model also rely on PTFs since it can simulate water fluxes in numerical models running on locally, regionally, and globally [20, 21]. There are a lot of methods and techniques to calculate PTFs. Mostly useful and simple formula of PTFs in developing country is based on bulk density only or particle size distribution and bulk density or soil organic matter [22]. However, PTFs prediction has low accuracy using soil texture only or bulk density only [20] because it is probably not applicable for wetland, swamps and desserts. It is wisely to calculate PTFs not only include bulk density and soil texture but also include soil organic matter in wetland, swamps, and desserts. Reliable and sufficient sampling in local scale also increases the accuracy of PTFs [23].

There are many methods that are widely applied to estimate K_s using PTFs such as Saxton and Rawls formula in (1986) and (2006). It firstly uses soil texture and bulk density to define K_s [24, 25]. Then, it is modified to include soil organic matter content in estimating K_s [9]. Since it includes bulk density and soil organic matter in PTFs, it is probably applicable for wetland such Barito Delta as the conclusion and suggestion in [23].

The hydraulic soil properties control the fluxes, that is, groundwater table, surface runoff, evapotranspiration, interflow, and whole water balances, in peatland [26]. Barito Delta is a peatland created from sediment deposition of river and marine landform in the southern of Borneo. This wetland is bounded by Barito and Kapuas Murung Rivers [27]. This Quadrangular shape of Barito Delta is poorly mapped [28]. Not only soil physical characteristics are rarely mapped, but also soil hydraulic characteristics of K_s are rarely measured, estimated, and analyzed in this peatland delta. It is time-consuming, difficult [29], expensive or not affordable [30], impractical [31], and nonaccessible place to measure K_s in large areas [29] and wetland [32, 33] such as in the wetland of Barito Delta.

The information of soil physical characteristics and K_s is important to understand the water cycle in wetland of Barito Delta. K_s is also basic information to model water interaction in groundwater soil and advances application studies. K_s is used to parameterize process-based hydrologic model because it shows shallow groundwater-surface water exchange process [11]. Therefore, the purpose of this paper is (a) to explore soil physical properties particularly soil fraction and soil textures, and soil organic matter in each landform, (b) to profile and characterize soil textures in the landform of Barito Delta, and (c) to estimate K_s from soil physical characteristics in Barito Delta landform.

2. Methods

Soil samples and electrical resistivity measurements are taken based on landform. Landform element is classified based on local surface shape, combination of surface shape and slope gradient, combination of surface shape, slope gradient, and contextual measure of relative landform position [34]. Landform map is generated and classified from Landsat imagery in 2008, soil type map, and slope map class. Landform map is validated with field check to Barito Delta. Soil type map is derived from soil map scale 1 : 250.000 in 1999. It is published by Bureau of Soil Research (locally called PUSLITANAK). Slope map is created from topography map scale 1 : 250.000 in 2000. Topography map is collected from Bureau for Geospatial Information (locally called BIG). Topography map is used because there is no cloud-free SRTM, so there is a mistake in mapping the terrain map.

2.1. Soil Samples. Soil sample for soil texture is taken using special hand auger bore for wetland. This sample is to analyze in laboratory to obtain particle size percentage (% sand, % silt, and % clay). The number of sample location for soil texture is 51 locations. In each location, soil sample is taken for 1 to 5 meter depth where for each one meter distance is being sampled. Only in a place where it reaches fine sand materials, it is not sampled until 5 m depth. It is because these fine sand materials are from the process of river sedimentation that occurs in the past, while the regolith or the bedrocks are hundreds of meter depths from this layer. Particle size and soil texture classification are defined applying USDA classification [35]. USDA triangle texture is also built in R software using soil texture Package [36].

Soil sample for bulk density (BD) analysis is taken using cylindrical ring (ϕ 5 cm). The number of sample location for BD is 28 sites. It is taken representatively at least for each landform except for Oxbow Lake. It is because (a) the depth of water in the basin of Oxbow Lake can reach 1 meter depth, (b) there is no access to reach this remote area, and (c) it is covered by water and grass. The value of bulk density is measured from laboratory testing. BD is taken only in land surface or land surface of first layer or at 1 meter depth. It is because (a) peatland is only on land surface, (b) the type of peatland is relatively similar from 1 to 3 meter depth so that the value of BD is relatively the same, and (c) a lot of sample locations are found fine sand materials in the 1^{st} to 2^{nd} meters depth.

Soil sample for soil organic matter (SOM) analysis is taken using special hand auger bore for wetland. The number of sample location for SOM is 10 sites that are taken representatively for each landform. In each location, soil sample is taken for 1 to 5 meter depth where for each one meter depth distance is being sampled. It is only limited sample taken for SOM because (a) it is rainy season where water depth above land surface can be 1 to 1.5 meters, (b) the study area gets influence from tidal activity and mostly inundated, and (c) it is not possible doing additional fieldwork with a lot of sampling sites at this moment for this research with limited time period.

2.2. Saturated Hydraulic Conductivity (K_s). K_s formula for Saxton and Rawls (1986) in [24, 25] expressed in equations (1) and (2) and Saxton and Rawls (2006) in [9] expressed in equations (3)–(9). In situ bulk density data (BD), soil organic matter content (SOM), clay (Cl), and sand (Sa) values are used to estimate K_s. θ_s (equation (1)) is estimated from in situ BD measurement, while θ_s (equation (4)) is estimated from in situ SOM measurement. K_s formula for Saxton and Rawls (1986) and Saxton and Rawls (2006) shows in equations (2) and (3) [9, 24]. However, Saxton and Rawls (2006) eliminate data with SOM >8%, Cl > 60%, and BD < 1%, and it makes it is not applicable in Barito Delta. It shows negative values of (θ_s–θ_{33}) so that there is no value of K_s. Therefore, K_s estimation uses Weynants et al. (2009) in [38] that apply soil texture, bulk density, and soil organic carbon (SOC) in calculation. SOC is from 58% of SOM according to USDA Natural Resources Conservation Service. The formula of K_s is shown in the following equation [25, 38]:

$$\theta_s = \phi = 1 - \frac{\text{BD}}{2.65}, \tag{1}$$

$$\begin{aligned}K_s = 24 \exp\Big(& 19.52348\, x\, \phi - 8.96847 - 0.028212\, x\, \text{Cl} \\ & + 0.00018107\, x\, \text{Sa}^2 - 0.0094125\, x\text{Cl}^2 \\ & - 8.395215\, x\, \phi^2 + 0.077718\, x\, \text{Sa}\, x\, \phi \\ & - 0.00298\, x\, \text{Sa}^2\, x\, \phi^2 - 0.019492\, x\, \text{Cl}^2\, x\, \phi^2 \\ & + 0.0000173\, x\, \text{Sa}^2\, x\text{Cl} + 0.02733\, x\text{Cl}^2\, x\, \phi \\ & + 0.001434\, x\text{Sa}^2\, x\, \phi - 0.0000035\, x\text{Sa}\, x\text{Cl}^2\Big),\end{aligned} \tag{2}$$

where θ_s is saturated soil moisture ($\text{cm}^3\,\text{cm}^{-3}$), ϕ is porosity, BD is bulk density ($\text{gr}\,\text{cm}^{-3}$), and K_s is saturated hydraulic conductivity (ms^{-1}).

$$K_s = 1930 * \left(\theta_s - \theta_{33}\right)^{(3-\lambda)}, \tag{3}$$

$$\theta_s = \theta_{33} + \theta_{(s-33)} - 0.097\,\text{Sa} + 0.043, \tag{4}$$

$$\begin{aligned}\theta_{33} = & -0.251\,\text{Sa} + 0.195\,\text{Cl} + 0.011\,\text{SOM} + 0.006\,(\text{Sa} * \text{SOM}) - 0.027\,(\text{Cl} * \text{SOM}) \\ & + 0.452\,(\text{Sa} * \text{Cl}) + 0.299 + \Big\{1.283 * \{-0.251\,\text{Sa} + 0.195\,\text{Cl} + 0.011\,\text{SOM} + 0.006\,(\text{Sa} * \text{SOM}) - 0.027\,(\text{Cl} * \text{SOM}) \\ & + 0.452\,(\text{Sa} * \text{Cl}) + 0.299\}^2\Big\} \\ & - \{0.374 * \{-0.251\,\text{Sa} + 0.195\,\text{Cl} + 0.011\,\text{SOM} + 0.006\,(\text{Sa} * \text{SOM}) - 0.027\,(\text{Cl} * \text{SOM}) + 0.452\,(\text{Sa} * \text{Cl}) + 0.299\}\} - 0.015,\end{aligned} \tag{5}$$

$$\begin{aligned}\theta_{(s-33)} = & \,0.278\,\text{Sa} + 0.034\,\text{Cl} + 0.022\,\text{SOM} - 0.018\,(\text{Sa} * \text{SOM}) - 0.027\,(\text{Cl} * \text{SOM}) \\ & - 0.584\,(\text{Sa} * \text{Cl}) + 0.078 + \Big\{0.636 * \{0.278\,\text{Sa} + 0.034\,\text{Cl} + 0.022\,\text{SOM} - 0.018\,(\text{Sa} * \text{SOM}) - 0.027\,(\text{Cl} * \text{SOM}) \\ & - 0.584\,(\text{Sa} * \text{Cl}) + 0.078\}\Big\} - 0.107,\end{aligned} \tag{6}$$

$$\lambda = \frac{1}{B}, \tag{7}$$

$$B = \frac{\{\ln(1500) - \ln(33)\}}{\{\ln(\theta_{33}) - \ln(\theta_{1500})\}}, \tag{8}$$

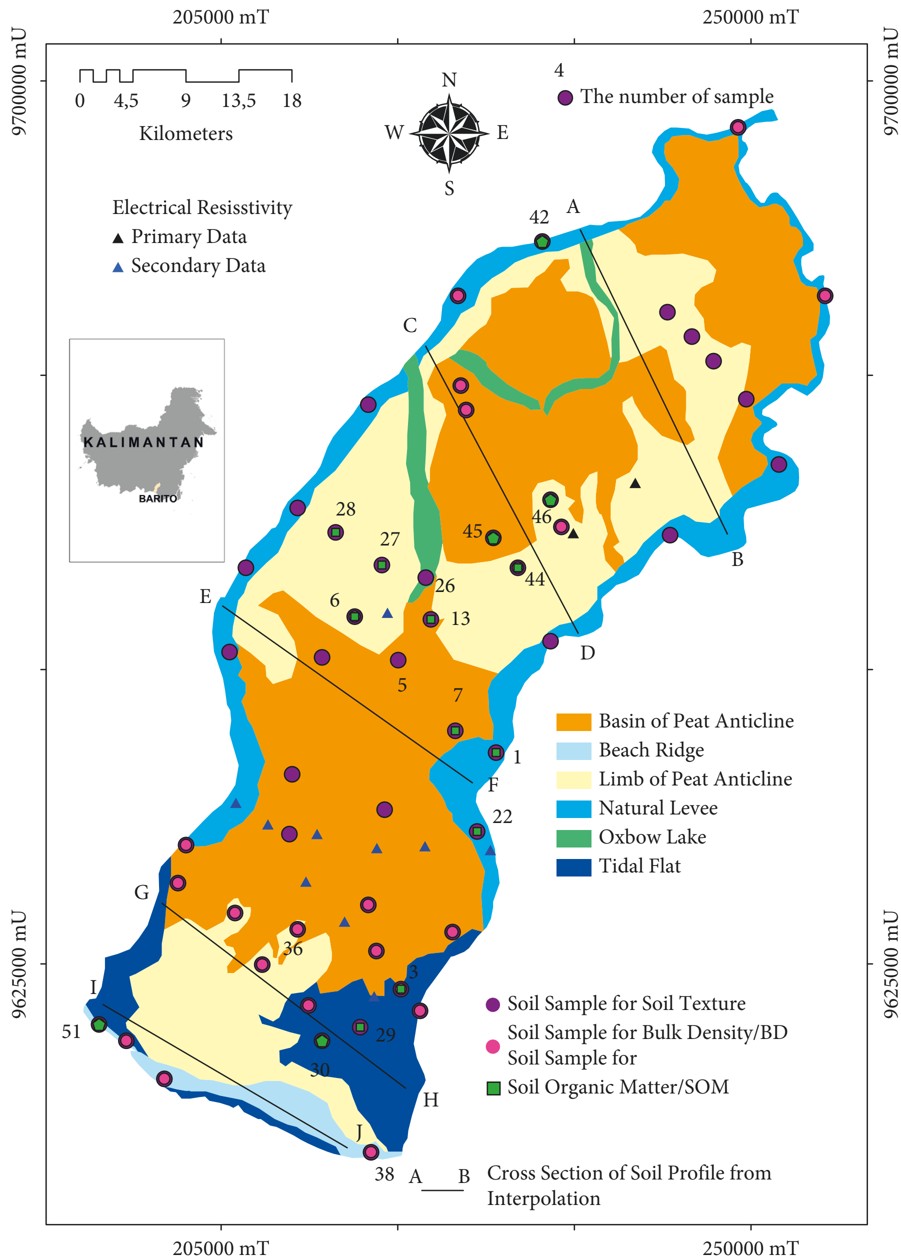

FIGURE 1: Location of soil samples and electrical resistivity measurement in landform of Barito Delta (source: modification of Arisanty [37]). The location of cross-section to describe in detail soil texture characteristics from interpolation.

$$\theta_{1500} = -0.024\,\mathrm{Sa} + 0.487\,\mathrm{Cl} + 0.006\,\mathrm{SOM} + 0.005\,(\mathrm{Sa} * \mathrm{SOM}) - 0.013\,(\mathrm{Cl} * \mathrm{SOM}) + 0.068\,(\mathrm{Sa} * \mathrm{Cl}) + 0.031$$
$$+ \{0.14 * \{-0.024\,\mathrm{Sa} + 0.487\,\mathrm{Cl} + 0.06\,\mathrm{SOM} + 0.005\,(\mathrm{Sa} * \mathrm{SOM}) - 0.013\,(\mathrm{Cl} * \mathrm{SOM}) + 0.068\,(\mathrm{Sa} * \mathrm{Cl}) + 0.031\}\} - 0.02, \quad (9)$$

where θ_s is saturated soil moisture (%v), SOM is soil organic matter content (%), K_s is saturated hydraulic conductivity (mmh^{-1}), λ is slope of logarithmic tension-moisture curve, and Cl and Sa are in %

$$K_s = \exp\,(1.9582 + 0.0308 * \mathrm{Sa} - 0.6142 * \mathrm{BD} - 0.01566 * \mathrm{SOC} * 1.72), \quad (10)$$

where SOC is soil organic carbon (%)

2.3. Bayesian Statistics. Spatial distribution of soil properties (% clay, % silt, or % sand) can be predicted and mapped with Bayesian statistics. From this interpolation, it can be constructed soil texture distribution along soil profile in landforms to explore soil characteristics in Barito Delta. It is because interpolation can be performed when data from soil sample (fixed depth of soil sample) and soil profile from fieldwork are available [39]. Several cross-sections (Figure 1) are selected representatively in the landform of Barito Delta.

This cross-section is used to help in explaining in detail the soil characteristics of Barito Delta.

The interpolation of soil physical characteristics is performed in R with gstat packages [40] applying Bayesian methods using geOR packages [41–43]. Noninformative priors are selected in this method because of limited information of the priors. Bayesian statistics formula shows in equation (11) that illustrates $p(\theta|Z)$ is posterior distribution, $p(\theta)$ is prior distribution, and θ is unknown parameters [44]. The Bayesian predictive distribution for soil physical characteristics in location s_0 is below.

$$p(Z((s_0)|Z)) = \int p(Z(s_0)|Z,\theta)p(\theta|Z)\mathrm{d}\theta. \quad (11)$$

A number of simulations to create the map are 1000 with spatial scale of 3 km × 3 km. This map is used to build cross-section of soil profile illustrating soil texture characteristics. Cross-validation procedure is applied to measure the quality of Bayesian to predict soil physical properties (% sand, % silt, and % clay). Cross-validation statistics of ME or mean error and RMSE or root mean square error is adapted from [45] in following equations:

$$\mathrm{ME} = \frac{1}{n}\sum_{i=1}^{n}(Zs_0 - Zs_\theta), \quad (12)$$

$$\mathrm{RMSE} = \sqrt{\frac{1}{n}\sum_{i=1}^{n}(Zs_0 - Zs_\theta)^2}, \quad (13)$$

where N is the number of observed values of soil physical characteristics (% clay, % silt, or % sand), Zs_0 is predicted value, and Zs_θ is observed value of soil physical characteristics (% clay, % silt, or % sand).

Since a lot of samples is taken not more than 3 m depth, the percentage of particle size for this untaken samples is following sample 51 in 3 m depth that consists of 75.57% of sand, 6.61% of silt, and 17.82% of clay. These percentages of untaken samples are only used for interpolation. The assumption of soil fraction in this sample is similar with fine sand materials from ancient sedimentation.

In this research, Bayesian statistics is applied and not inverse distance weighting (IDW) although the model of Bayesian statistics is fitted with pure nugget. It is because pure nugget model could not be rejected although weaker spatial dependences are occurred in soil mapping [46]. This pure nugget effect exists perhaps due to horizontal sampling distance condition [47]. Bayesian statistics with pure nugget effect also is selected because transfer error values of interpolation applying Bayesian statistics show lower RMSE compared with IDW (Table 1). The RMSE equation of transfer error value is due to interpolation shown in equation (14). This formula is as follows [48, 49]. The values of soil fraction for observed values can be completely shift while using IDW compared with Bayesian statistics (Table 1). It can be shown below in Table 1 that illustrates error values comparison of RMSE values applying IDW and Bayesian statistics interpolation.

Table 1: The values of RMSE (%) for transfer error interpolation of soil fraction applying Bayesian statistics and IDW.

Soil depth (m)	RMSE Bayesian statistics			RMSE IDW		
	Sand	Silt	Clay	Sand	Silt	Clay
1	1.94	8.82	10.10	22.13	15.41	35.60
2	1.97	10.99	12.54	23.04	14.32	32.29
3	25.79	11.79	18.07	41.87	19.58	33.73
4	20.55	13.37	15.02	49.21	24.54	28.23

$$\mathrm{RMSE} = \sqrt{\frac{1}{n}\sum_{i=1}^{n}(x_0 - x)^2}, \quad (14)$$

where n is the number of sample or observed values of soil physical characteristics (% clay, % silt, or % sand), x_0 is interpolation values of soil physical characteristics (% clay, % silt, or % sand) applying Bayesian statistics or IDW, and x is observed value of soil physical characteristics (% clay, % silt, or % sand).

3. Result and Discussion

3.1. Soil Physical Characteristics. Soil texture characteristics are illustrated representatively applying USDA triangle texture diagram in Figures 2 and 3. It is selected to a sample that has BD and SOM data in Figure 1. Complete USDA triangle texture for all samples can be seen in [50]. Clay and silty clay are the dominant soil texture in 1 to 2 meter depth in the peatland of Barito Delta (Figure 2). The percentage of clay and silt particles has majority distribution in the landforms of Barito Delta. Mostly, the percentage of clay particle is larger than silt particle in the magnitude of ~10%. Natural Levee has the largest clay content in the soil. Sand particle has the lowest content in 1 to 2 meter soil depth. The lowest percentage of sand particle can be ~0.08%. The percentage of sand particle is larger in Tidal Flat and Limb of Peat Anticline in 1 to 2 meter depth. Sandy loam is the major soil texture in the 3rd to 4th meter of soil depth. It is because sand particle percentage increase along soil profile. Natural Levee has the lowest content of sand particles in these depths.

Clay is the majority soil texture in 1 to 2 meter along soil profile in the landform of Barito Delta (Figure 3). The percentage of clay particle can be more than 60%. Natural Levee has the largest content of clay particle ~89% in the 1st meter depth. Tidal Flat and Basin of Peat Anticline have larger clay content in the 2nd depth compared with Natural Levee and Limb of Peat Anticline. Clay is soil texture in Natural Levee and Limb of Peat Anticline in 3 meter depth along soil profile, while Tidal Flat and Basin of Peat Anticline are sandy loam. Soil texture tends to be heterogeneous in 4 meter depth along soil profile in Barito landform. It is probably because sedimentation process is not as active as in the 1st meter of soil depth. The percentage of soil particle within soil depends on infiltration process where water can carry soil fraction downward. Moreover, soil-clay decreases consistently with changes of soil structure along soil profile [51].

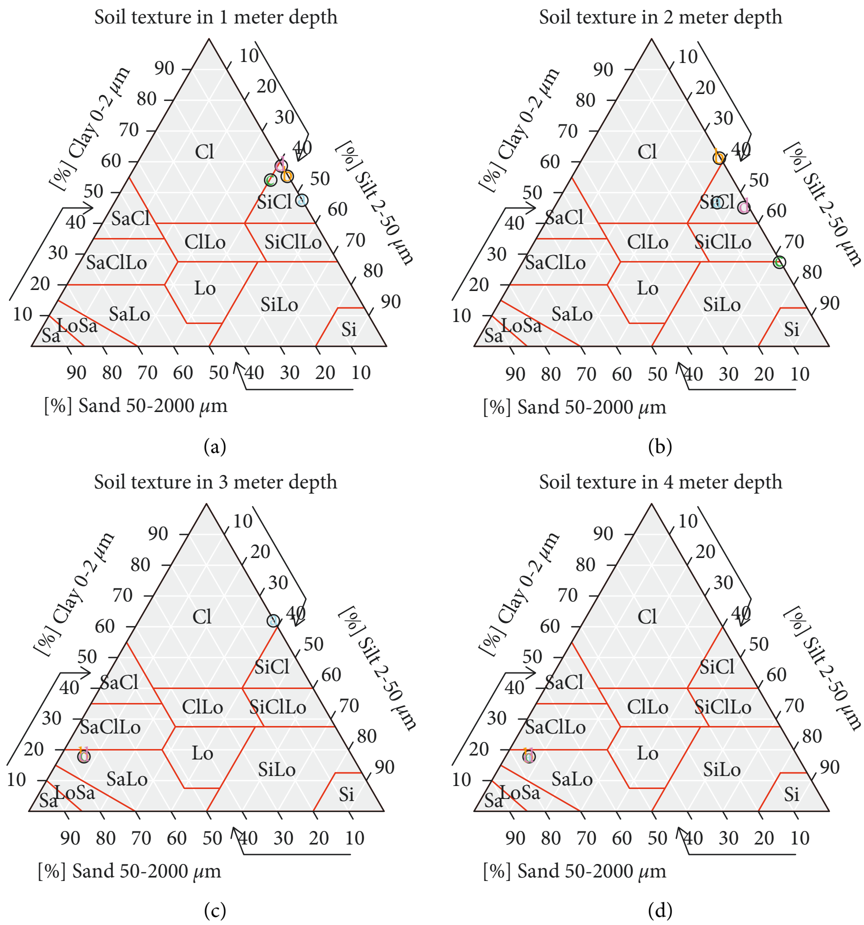

Figure 2: USDA triangle soil texture in 1st to 4th meters depth in the landform of Barito Delta. Soil texture in each landform indicates with color alphabet, that is, (a) with light blue color, Tidal Flat (Sample No. 3); (b) with orange color, Natural Levee (Sample No. 22); (c) with green color, Limb of Peat Anticline (Sample No. 6); (d) with violet color, Basin of Peat Anticline (Sample No. 13).

Clay is the most common and dominant soil fraction in various landforms in Barito Delta (Figure 4). Sand particle is very low and almost can be neglected due to limited content in the soil of Delta. It is because the minimum value of sand particle can be ~0.01%, especially in 1 to 2 meter soil depth so that percentage of sand particle only is written in legend of the figure, while percentage of clay and silt fraction is shown in graphic of figure (Figure 4). In Natural Levee, clay contains around 85% with an abruptly decreasing along profile of soil depth. In contrast to silt fraction, silt contains around 10% with an increasing along profile of soil depth. Both of them have comparable percentage content within soil at 5 m depth. It is because both of clay and silt particles have low percentage within the soil, while sand is the dominant soil particle after 5 m depth. These soil characteristics of Natural Levee are similar with Limb of Peat Anticline.

In Basin of Peat Anticline, the soil characteristics are different with other landforms (Figure 4). Clay particle contains much higher compared with silt and sand particles. The clay particle in the soil does not decrease continuously with the depth of soil. It is because in the basin frequently occurs sedimentation. Water and its mineral content have more time to stay at the basin to infiltrate further downward along profile so that the clay contents in the soil depend on each process of sedimentation, infiltration rate, and available soil mineral particle in certain time.

The soil characteristics are in contrast to each other in Oxbow Lake and Beach Ridge (Figure 4). Clay contents around 55% with abruptly increasing along profile in Oxbow Lake, while in Beach Ridge decreasing. It is because river mostly carries clay particles in sedimentation process in Oxbow Lake, while sea water mostly carries sand particles in sedimentation process in Beach Ridge. Soil samples in Beach Ridge and Oxbow Lake are only taken until 2 meter depth because fine sand material from ancient sedimentation is found below 2 m depth. It is as indication there is sedimentation that occurs in the past.

Tidal Flat also has specific soil characteristics compared with other landforms (Figure 4). The fraction of sand particle largely contents in the soil of Tidal Flat compared with other landforms. It is because Tidal Flat is generally dominated with sand particles [52]. This landform occurs both sedimentation from sea water and sedimentation from river. The sea water sedimentation is more active than river water so that sand and clay including silt particles are comparable. Barito estuary is also controlled by tidal currents during dry season [28].

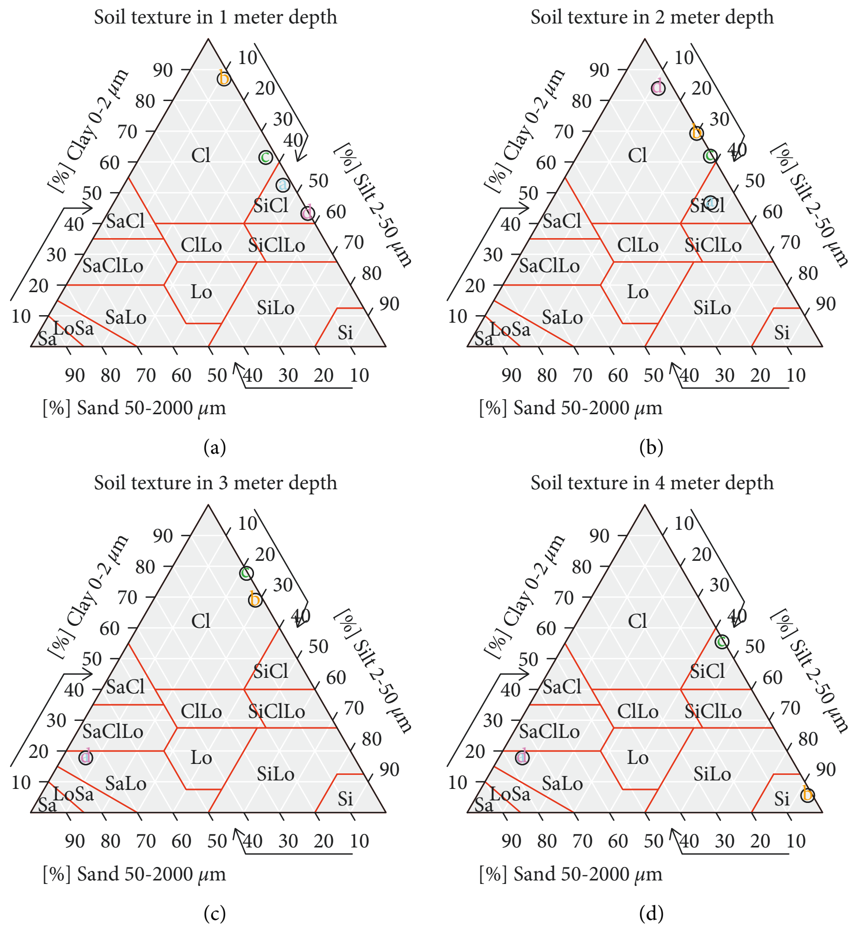

Figure 3: USDA triangle soil texture in 1st to 4th meters depth in the landform of Barito Delta. Soil texture in each landform indicates with color alphabet, that is, (a) with light blue color, Tidal Flat (Sample No. 29); (b) with orange color, Natural Levee (Sample No. 1); (c) with green color, Limb of Peat Anticline (Sample No. 44); and (d) with violet color, Basin of Peat Anticline (Sample No. 7).

Electrical resistivity measurement is helpful to map soil layers [53] and soil structure [54]. In this research, we use electrical measurement to estimate soil depth and soil texture. Since the landscape is challenging, we only take two measurements in the field as primary data. It is to complete and support the information of soil samples and secondary data of electrical resistivity measurement from Hehanussa et al. [55]. Wenner method is applied to measure electrical resistivity. Data are plotted on respective graphs, and the values are calculated in this method. Vertical electrical sounding is recorded from the changes of resistivity with depth and correlate with geological information to infer the depths and resistivity of the present layers [56]. RES2DINV software is used to obtain the visualization of resistivity model.

The electrical resistivity 3D imaging is situated in Limb of Peat Anticline (Figure 5). It also confirms that clay is the dominant soil fraction in Barito Delta. This peatland also has mud along soil profile. It can be found until the 25 m depth with resistivity value of 5.23 Ωm. The next depth of soil profile can be found clay texture, followed with sand texture. This sand texture confirms there is ancient sedimentation below 10 meter depth with resistivity value of 11.5–25.1 Ωm. It is an agreement with [57] that electrical resistivity can also help to estimate peat basin structure and mineral sediments.

Soil organic matter content (SOM) is mostly concerned in the peatland because of organic compound abundances in the soil. Soil is mostly not peaty soil in Barito Delta since the values of SOM are mostly less than 4%. Only Natural Levee and Tidal Flat (Figure 6(b)) have peaty soil because the values of SOM are more than 10% [58]. SOM percentage changes along soil profile in Barito Delta (Figures 6(a) and 6(b)). It is an agreement with [59] that SOM should change steadily down soil profile as a result of peat forming process. It can be because of land use effect, drainage effect, and long-lasting decomposition [60] so that the magnitude of changes should be different. The changes of SOM are mostly decrease abruptly from 1st depth to 2nd depth of soil, while in 3rd and 4th depth mostly not significantly change as occurs in 1st to 2nd depth. It is probably because 1st to 2nd depth get intensive influence of decomposition including infiltration, drainage, and land use condition. There are very sharp changes of SOM in Natural Levee and Tidal Flat (Figure 6(b)) from 2nd to 3 m soil depth because 1st soil depth is peaty soil with more than 10% of SOM, while 3rd *m* depth 3% of SOM.

The cross-validation of soil fraction mapping in each soil depth applying Bayesian statistics shows in Table 2. The ME values are mostly low ranging from 0.02 to 0.05. Only in the first 1 meter depth has ME values of −0.20 for clay fraction

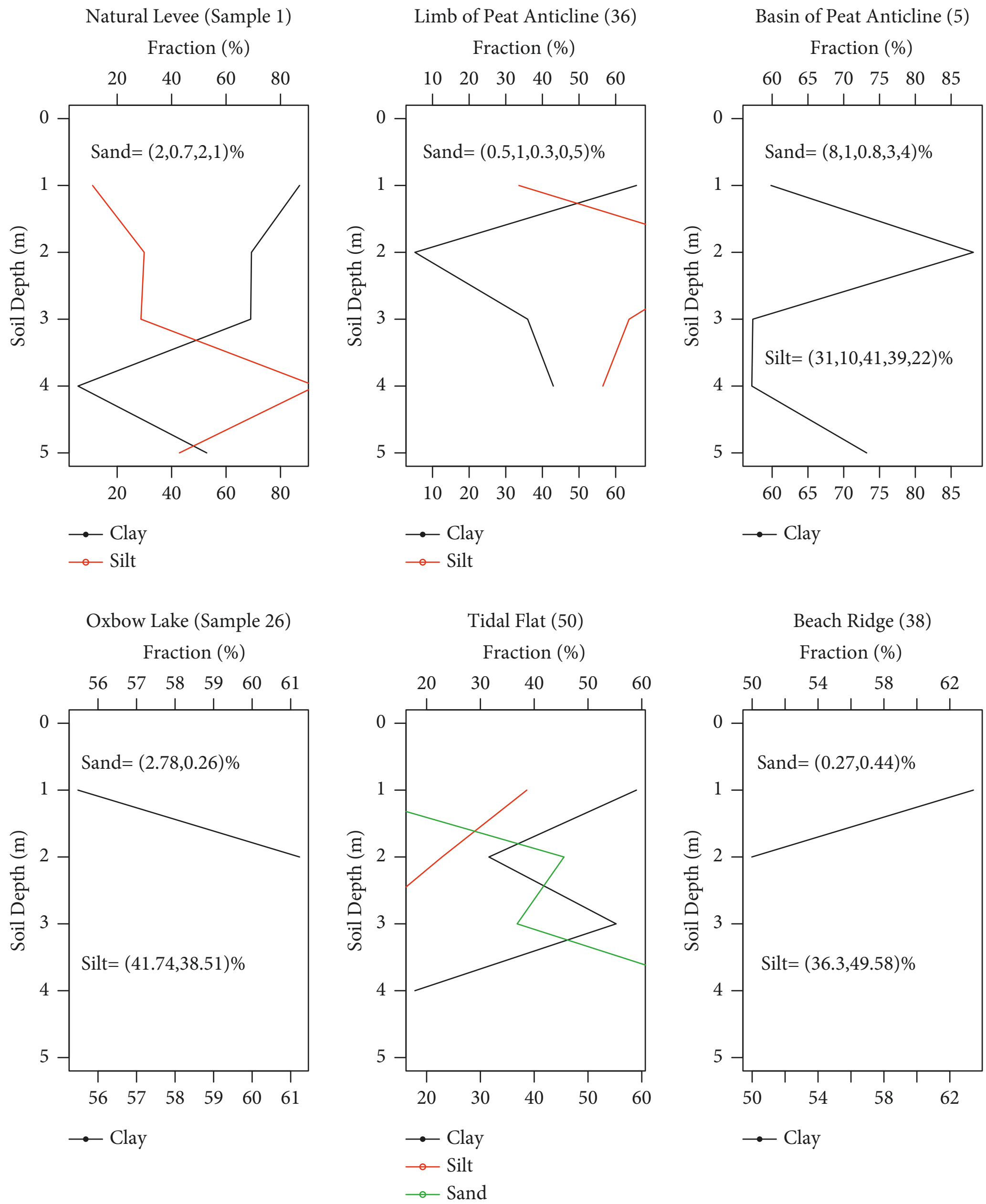

Figure 4: The percentage of soil fraction vs soil depth in various landforms of Barito Delta. The low content of certain soil particle fraction, that is, sand fraction, is mostly not able to shown to all graphics in this figure because the percentage value is too low compared to other fractions so that its value is written in the text in each graphic of figure. For example, sand = (2, 0.2, 4, 8)% means percentage of sand fraction in 1st depth is ~2, 2nd depth is ~0.2, 3rd depth is ~4, and 4th depth is ~8%.

mapping and the 4 m depth that has ME values of 0.50 for sand fraction mapping. It is probably because both of them have largest fractions of certain particle in those soil depths; that is, clay fraction is the largest particle in 1 m depth and sand fraction is the largest particle in 4 m depth. The RMSE values are also low if it is compared with the values of soil fraction percentage.

Generally, clay texture is existing in 1 to 2 meter depth of soil profiles in the landforms of Barito Delta (Figure 7). As soil profile is going deeper, the courser soil particle is existing in 3 to 4 meter depth such as loamy sand and sandy loam. It is because sandy loam is a transitional texture that moisture retention properties change from course to medium soil texture [61]. Heterogeneous soil texture is existing in the landforms that are influenced by river water and sea water sedimentation. It can be seen in soil profile cross-section of AB and CD. In soil profile AB and CD, Basin of Peat Anticline has homogeneous soil textures because it is close to Limb of Peat Anticline that both of these landforms are influenced by sedimentation processes of river water. Clay loam texture is usually existing after clay texture in the next depth of soil profile. Usually, it is an indication that river sedimentation is dominant process to the landform than sea water. For example, soil textures are continuously clay, clay

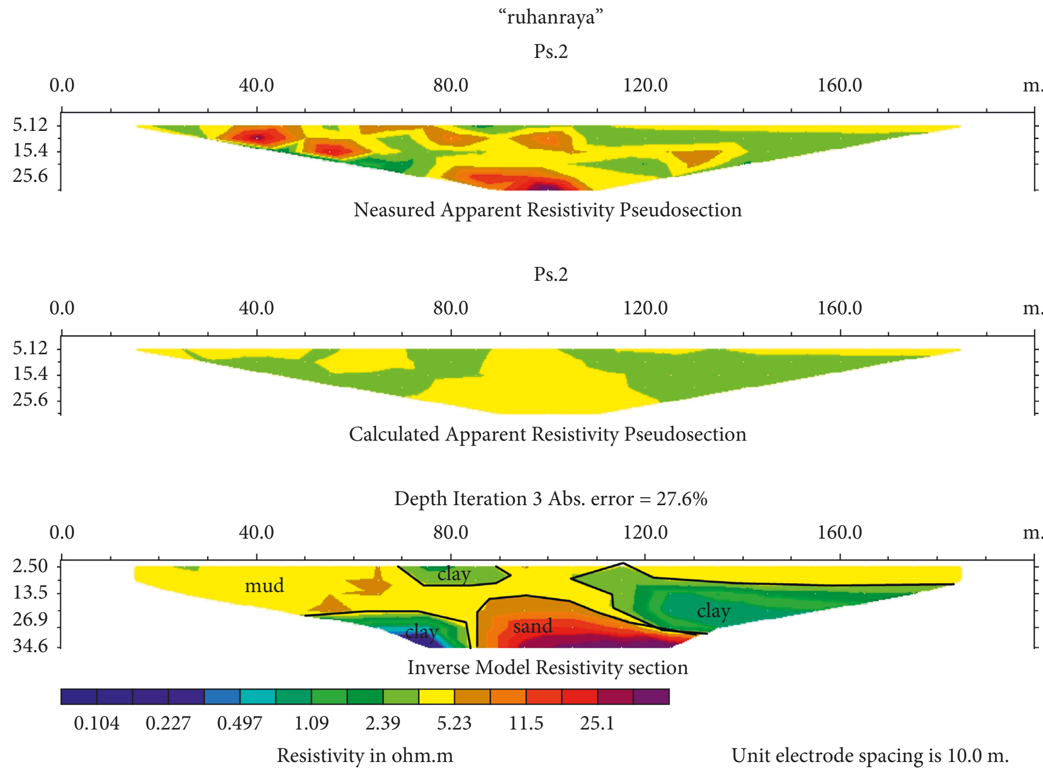

Figure 5: Electrical resistivity 3D imaging at Limb of Peat Anticline (source: primary data, 2012).

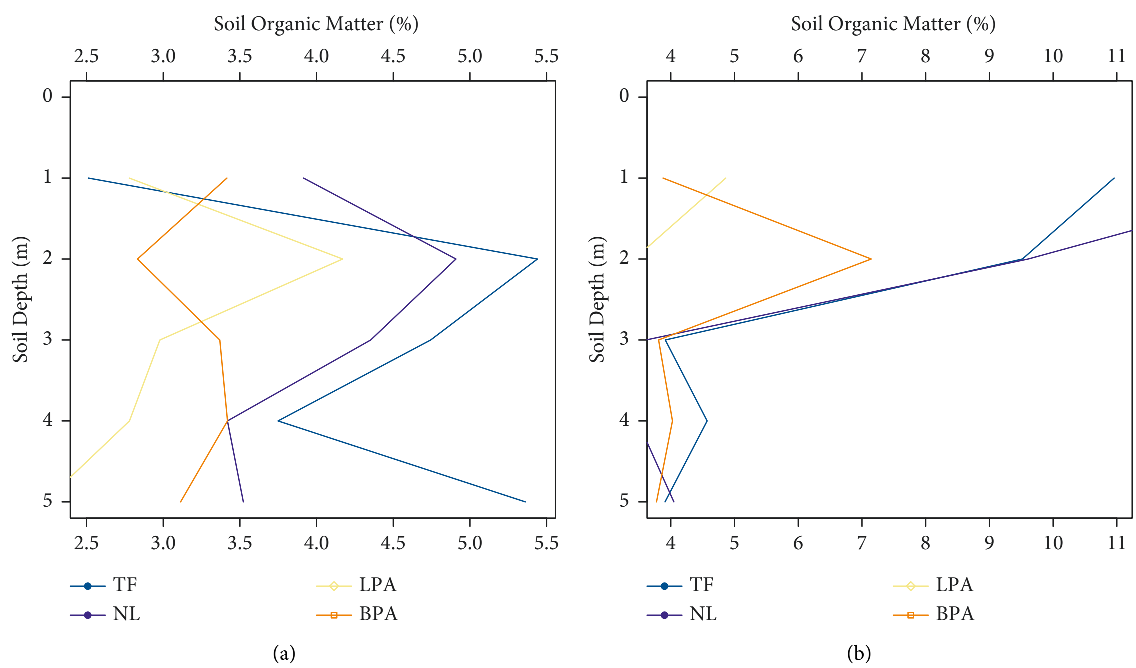

Figure 6: Soil organic matter (SOM) along soil profiles in the landform of Barito Delta. TL is tidal flat, NL is natural levee, LPA is limb of peat anticline, and BPA is basin of peat anticline.

loam, and sandy clay loam as going deeper along soil profile in the landforms of Basin of Peat Anticline and Limb of Peat Anticline in AB. It is an opposite with Limb of Peat Anticline that is bordered with Natural Levee. These landforms are influenced both from river water and sea water so that soil texture along depth of soil profile is heterogeneous. For example, soil textures are continuously silty clay, clay, sandy loam, and loamy as going deeper along soil profile in EF.

Clay is the soil texture in 1 meter depth along soil profile in Barito Delta in cross-section GH and IJ

Table 2: Cross-validation of ME and RMSE of soil fraction mapping in each soil depth applying Bayesian statistics.

Depth (m)	Soil fraction (%) Clay		Silt		Sand	
	ME	RMSE	ME	RMSE	ME	RMSE
1	−0.20	12.93	−0.00	11.00	−0.00	1.80
2	−0.05	15.61	−0.00	15.15	−0.04	13.86
3	0.04	30.32	0.00	20.65	−1.41	45.77
4	0.00	25.13	−0.00	25.33	0.21	41.46

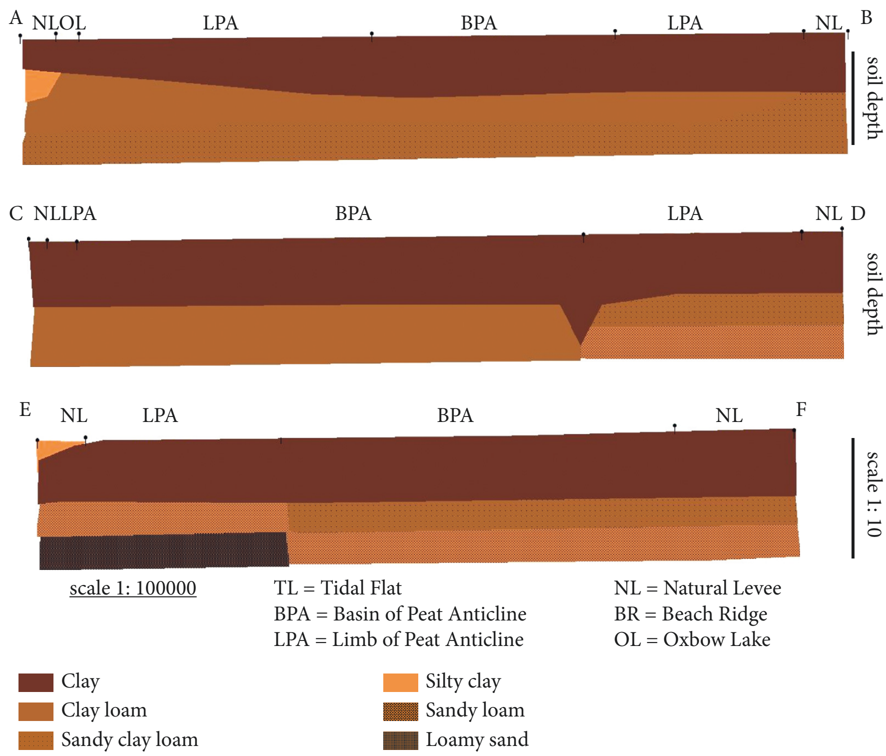

Figure 7: Soil profile for cross-section AB, CD, and EF in Barito Delta. The location of cross-section AB, CD, and EF can be checked in Figure 1. It is constructed based on the result of interpolation of soil fraction applying Bayesian statistics. Horizontal axis is land surface, while soil depth is vertical axis. Horizontal and vertical scales are different for layout configuration only.

(Figure 8). These cross-sections have much more intensive sea water activity since it is bordered with sea water. Tidal activity is more active controlling sedimentation. It can be seen there are Beach Ridge and Tidal Flat in cross-section GH and IJ. Since sea water sedimentation is more intensive than river water, silty clay texture is existing in 2 m depth below clay texture in 1 m depth. The indication of intensive sea water activity can be seen also from the existing of loamy sand texture in 3 to 4 meter depth in GH and IJ. This courser texture of loamy sand is not available in AB and CD because there is no sea water process and sea water is far from landforms in AB and CD. EF is more close to sea water than CD or AB so that loamy sand is existing in Natural Levee and its adjacent landform, Limb of Peat Anticline (Figure 7). It is because tidal activity has more influence to GH and IJ than AB and CD. Different processes and sediment activity surrounding river banks can influence clay-silt or sand-silt dominant fraction in the soil of peatland [62].

3.2. Saturated Hydraulic Conductivity (K_s). To explain in detail, only several samples of K_s values are displayed. The values of K_s generally increase along the depth of soil profile in Natural Levee applying Saxton and Rawls (1986) as shown in Figure 9. The value of K_s increases continuously with the depth as the sand particle contain much higher at deeper soil profile. It is an opposite with [63] that K_s values decrease along the depth of soil profile. There is an abrupt change of K_s values from 3 to 4 m depth because of the larger values of sand particles as going deeper from land surface of Barito Delta. The values of K_s above 3 m depth are less than 1 ms^{-1} since larger portion of clay content in the soil. In Sample 42, the K_s values are continuously 0.03, 0.1, 0.1, and 0.75 ms^{-1} from 1 to 4 meter depth.

The complex process that occurs in Limb of Peat Anticline is leading to different behaviors of K_s values along soil profile (Figure 9). The rate of sedimentation process is also controlled by slope in Limb of Peat Anticline. This landform is not as flat as Natural Levee, Basin

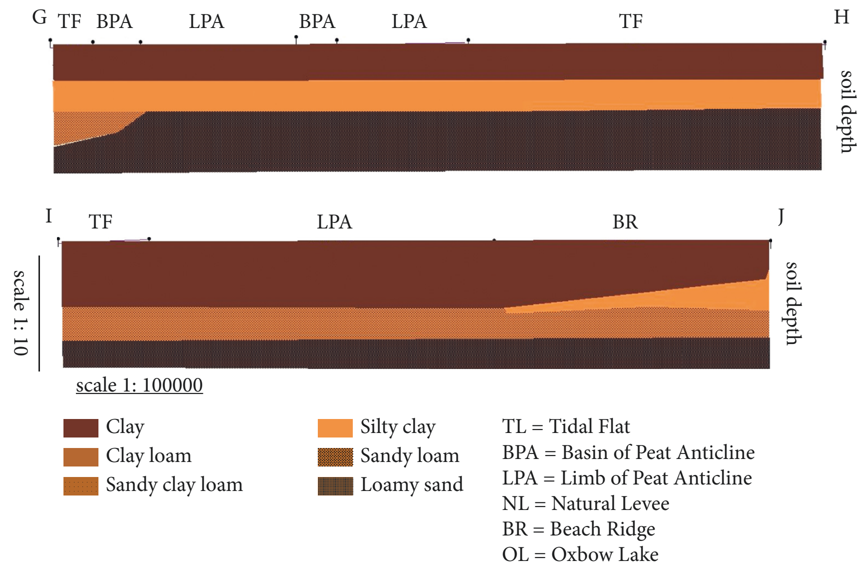

Figure 8: Soil profile for cross-section GH and IJ in Barito Delta. The location of cross-section GH and IJ can be checked in Figure 1. It is constructed based on the result of interpolation of soil fraction applying Bayesian statistics. Horizontal axis is land surface, while soil depth is vertical axis. Horizontal and vertical scales are different for layout configuration only.

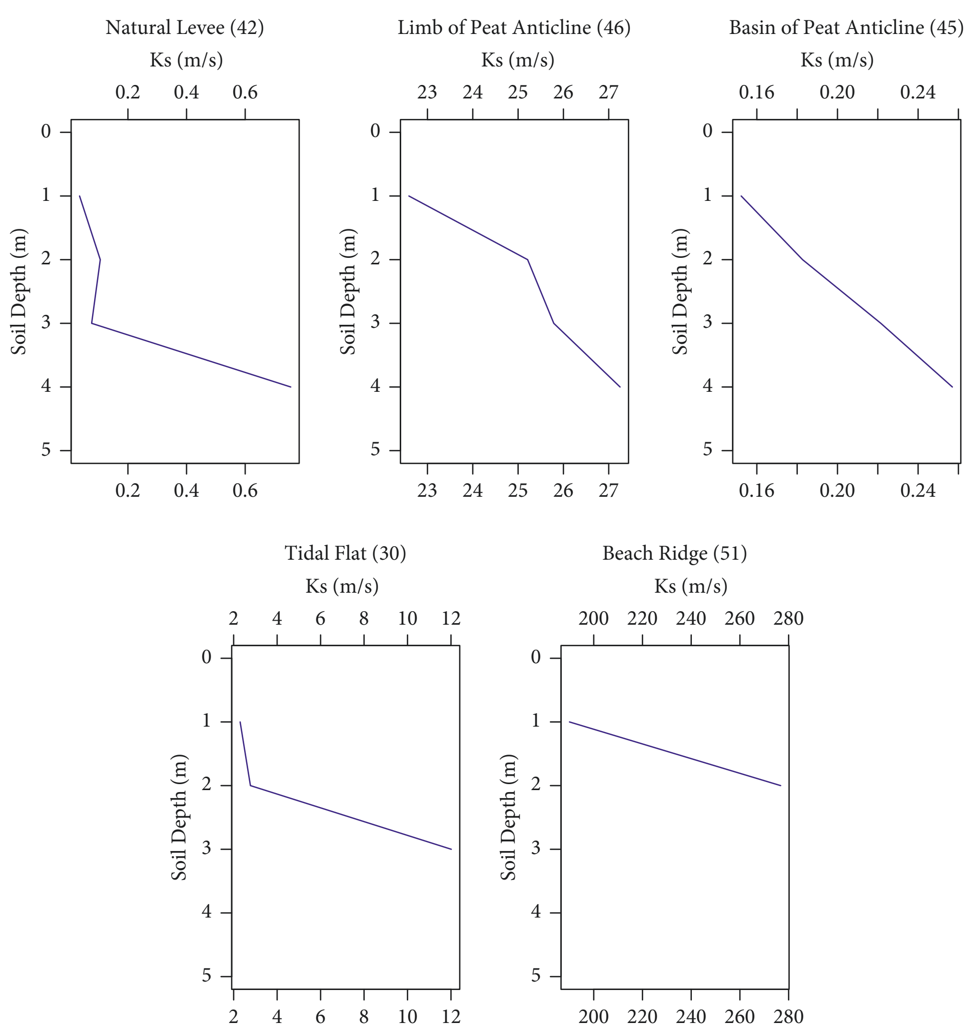

Figure 9: The values of K_s profile along soil depth in different landforms in Barito Delta applying Saxton and Rawls (1986).

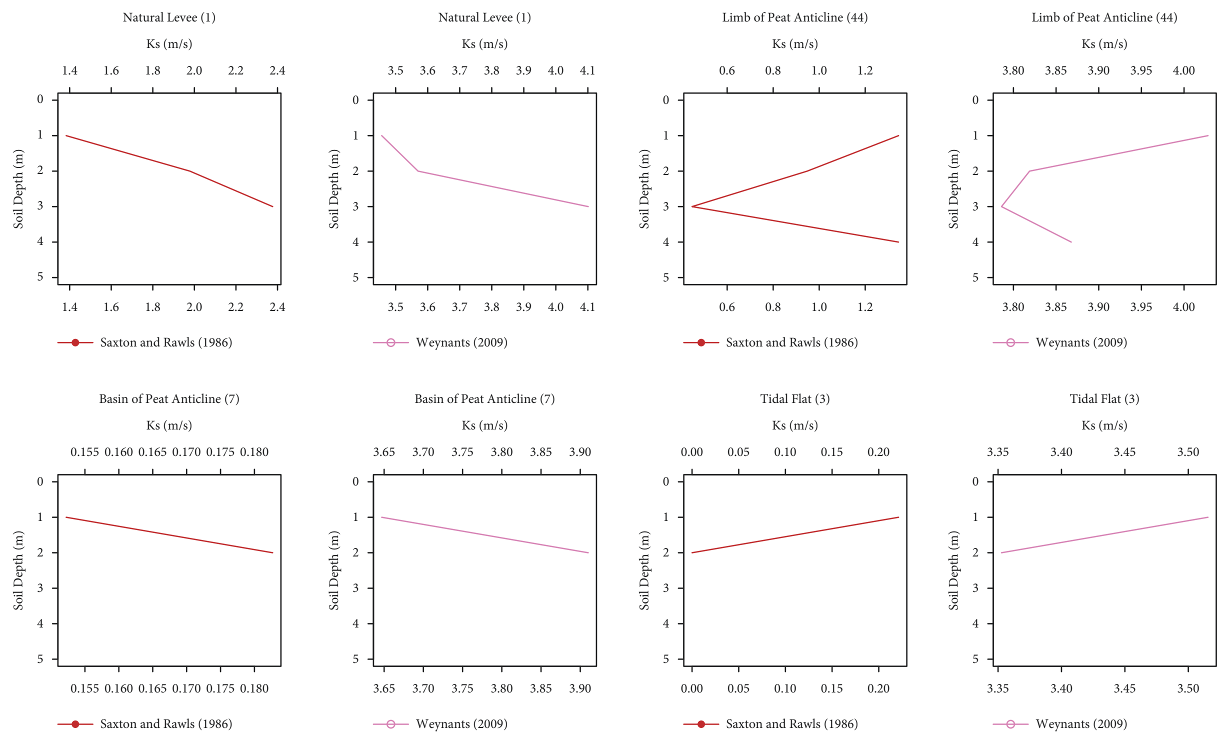

FIGURE 10: Comparison of K_s profile along soil depth in different landforms in Barito Delta applying Saxton and Rawls (1986) vs Weynants et al. (1999).

of Peat Anticline, and Tidal Flat so that mostly water can flow and easily carry fine particle of clay and leaving coarser particle of sand or silt in Limb of Peat Anticline. This courser particle of sand or silt is leading to larger K_s values in Limb of Peat Anticline compared to in Natural Levee and Basin of Peat Anticline. In the 1st depth of soil, the K_s values are more than $10\,\mathrm{m\,s^{-1}}$ in Limb of Peat Anticline.

K_s values are larger in Basin of Peat Anticline compared with Natural Levee (Figure 9). As a basin, it is a location where a lot of materials from sedimentation process mostly stay in this area so that courser particle can give contribution to make this landform has larger K_s than Natural Levee. But, the K_s characteristics in Basin of Peat Anticline are similar with Natural Levee that the K_s values increase along the depth of soil profile. In Sample 42, the K_s values are continuously 0.03, 0.1, 0.1, and $0.75\,\mathrm{ms^{-1}}$ from 1 to 4 meter depth.

K_s values are large in Tidal Flat (Figure 9). This landform is mostly influenced by sea water. Courser particles, that is, silt and sand, are largely content within the soil in this landform. It is similar with Beach Ridge that has more intensive sea water activity compared to Tidal Flat landform. It is leading to very large values of K_s in Beach Ridge than in Tidal Flat. In Tidal Flat, the values of K_s also increase along the depth of soil profile. The values of K_s continuously from 1st depth to 3rd depth of Sample 30 are 2.3, 2.77, and $12.01\,\mathrm{m\,s^{-1}}$. The values of K_s increase abruptly from 2nd depth of soil to the 3rd of soil from 2.77 to $\sim 12\,\mathrm{m\,s^{-1}}$. It is because the sand particle increases along the depth and it is close to the 4th depth of soil where it is found fine sand material from ancient sedimentation.

The values of K_s from Saxton and Rawls (1986) are lower compared with Weynants et al. (2009) in all landforms in Barito Delta (Figure 10). However, Weynants et al. (2009) include soil organic matter in estimating K_s, but it does not input clay fraction. It is because peatland characteristics are not only from soil organic matter and soil organic carbon but also from clay vs sand fractions. The pattern of K_s values is almost similar for both methods that K_s values decrease in downward direction. Only in Limb of Peat Anticline, the value of K_s decreases downward to 3rd depth of soil and slightly increases to 4th soil depth. The pattern of K_s values is similar in Basin of Peat Anticline and Tidal Flat that K_s values have negative or positive correlation with soil depth in downward direction. It is probably because both landforms are flat compared with Natural Levee or Limb of Peat Anticline. The discrepancy values of K_s from both methods appear largely in Basin of Peat Anticline and Tidal Flat. Clay and silt fractions mostly have comparable values in the soil of both landforms.

Saxton and Rawls (1986) are applicable to estimate K_s values in Barito Delta. It is because the values of K_s estimation are close to K_s values from measurement based on previous studies in peatland. The K_s values are 0.7×10^{-5} to $1.3 \times 10^{-2}\,\mathrm{ms^{-1}}$ in peatland [64], and 7.16×10^{-6} to $2.69 \times 10^{-2}\,\mathrm{ms^{-1}}$ K_s values variation [65]. K_s values according to Weynants et al. (2009) tend to have very small variation and tend to have overestimation. K_s values are varied between $3\,\mathrm{ms^{-1}}$ and $4.3\,\mathrm{ms^{-1}}$, while Saxton and Rawls (1986) are from 8×10^{-5} to 8×10^{5} depending on percentage of sand vs clay and soil depth. The high value of K_s is only in landform near sea water that abundances with sand particles.

4. Conclusion

Clay is the major soil particles in the landforms of peatland of Barito Delta. Clay fraction is mostly more than 60% existing within the soil. Clay content can reach more than 80% if the recent river sedimentation is intensive such as in Basin of Peat Anticline and Natural Levee. Mostly, sand particles are less than 1% available in the soil. In case of higher values of sand particles within 1 to 2 depths of soil, it is because the dominant sedimentation process occurs in certain landform. Sand particles that have larger percentage along soil profile in the landform after 2 or 3 meter depth are from ancient river sedimentation that occurs in the past. Sea water also influences clay content in the soil of Barito Delta. Mostly, clay is less available in soil fraction in the landform that is affected by sea water. That is why in the landform that is affected by sea water and river water can have heterogeneous soil texture along soil profile depth. It is because both sedimentations from sea and river determine the circulation of soil fraction in the soil. Silty clay and loamy sand mostly can be used as the signal, and there is sea water activity that influences the landforms such as Tidal Flat and Beach Ridge.

Soil organic matter (SOM) is mostly ranging from 2 to 3%, which contains in soil of Barito Delta. Only a few samples show peaty soil. It is because a lot of peatland areas are converted to agricultural and settlement areas since long time ago. SOM percentage has negative correlation with soil depth from 1st to 2nd depth that SOM relatively decreases along soil depth. SOM values have relatively stable values to the next downward depth.

Since K_s values from Saxton and Rawls (1986) are more applicable in Barito Delta than Weynants et al. (1999), the description of K_s values in this section is based on Saxton and Rawls (1986). The dominant soil fraction is clay particle, and the values of K_s are low in each landform, especially in 1 meter depth along soil profile. The value is ranging from 1.10^{-5} to $1.00\,\mathrm{m\,s^{-1}}$ in 1 m depth. Only in Limb of Peat Anticline, that K_s values can be more than $10\,\mathrm{m\,s^{-1}}$. It is probably the fine particle of clay flows down to the basin leaving course particle in Limb of Peat Anticline so that in basin has lower values of K_s compared to in limb. In the depth below 2 m depth, the Ks values are heterogeneous depending of major soil fraction in landform. It is because soil fraction (clay, silt, and sand) existing in the soil depending on intensive sedimentation process occurs in each landform. The value of K_s abruptly increases after 2 or 3 m depth as it reaches fine sand particle from ancient sedimentation.

It is recommended to measure BD in every soil depth to measure K_s values. The remote area, big rivers, no available pathway, and road are a big challenge to perform this measurement. From one sample to other samples, often we should be taken by boat. It also takes much time to perform measurement from one sample to other samples. Fieldwork mostly cannot be done in rainy season since the inundated water can be 1 to 1.5 meter above land surface. Additional analysis of soil physical characteristics also can be done to validate the value of K_s. Advanced research should be done further to this area.

Data Availability

The data supporting this article are datasets, which has been cited in [50].

Conflicts of Interest

The authors declared that they have no conflicts of interest.

Authors' Contributions

NR conceptualized the data; DA and NR developed the methodology and performed formal analysis; NR provided software and performed data curation. DA performed investigation, provided resources, and contributed to project administration. DA and NR performed validation. NR wrote original draft of the manuscript; DA did funding acquisition, and reviewed and edited the manuscript. DR reviewed the manuscript.

Acknowledgments

The authors would like to thank fieldwork team and Lambung Mangkurat University for granting permission and research funding.

References

[1] T. J. Jackson, "Remote sensing of soil moisture: implications for groundwater recharge," *Hydrogeology Journal*, vol. 10, no. 1, pp. 40–51, 2002.

[2] V. K. Phogat, V. S. Tomar, and R. Dahiya, *Soil Physical Properties*, Indian Society of Soil Science, New Delhi, India, 2015.

[3] C. García-Gutiérrez, Y. Pachepsky, and M. Á. Martín, "Technical note: saturated hydraulic conductivity and textural heterogeneity of soils," *Hydrology and Earth System Sciences*, vol. 22, no. 7, pp. 3923–3932, 2018.

[4] M. C. Lukenbach, C. J. Spencer, C. A. Mendoza, K. J. Devito, S. M. Landhäusser, and S. K. Carey, "Evaluating how landform design and soil covers influence groundwater recharge in a reclaimed watershed," *Water Resources Research*, vol. 55, no. 8, pp. 6464–6481, 2019.

[5] J. Karki, U. K. Mandal, C. L. Chidi, J. Dahal, N. R. Khanal, and R. H. Pantha, "An analysis of hydraulic properties of soil based on soil texture in Chiti areas of lamjung district in Nepal," *Geographical Journal of Nepal*, vol. 11, pp. 63–76, 2018.

[6] M. Bonsu, "A study of a texture-based equation for estimating the saturated hydraulic conductivity of an Alfisol in the Sudan savannah ecological zone, Ghana," *Hydrological Sciences Journal*, vol. 37, no. 6, pp. 599–606, 1992.

[7] S. Mishra, J. C. Parker, and N. Singhal, "Estimation of soil hydraulic properties and their uncertainty from particle size distribution data," *Journal of Hydrology*, vol. 108, pp. 1–18, 1989.

[8] P. R. Chaudhari, D. V. Ahire, V. D. Ahire, M. Chkravarty, and S. Maity, "Soil bulk density as related to soil texture, organic matter content and available total nutrients of coimbatore soil," *International Journal of Scientific and Research Publications*, vol. 3, 2013.

[9] K. E. Saxton and W. J. Rawls, "Soil water characteristic estimates by texture and organic matter for hydrologic

solutions," *Soil Science Society of America Journal*, vol. 70, no. 5, pp. 1569–1578, 2006.

[10] B. Usowicz and J. Lipiec, "Spatial variability of saturated hydraulic conductivity and its links with other soil properties at the regional scale," *Scientific Reports*, vol. 11, no. 1, p. 8293, 2021.

[11] K. S. Gootman, E. Kellner, and J. A. Hubbart, "A comparison and validation of saturated hydraulic conductivity models," *Water*, vol. 12, no. 7, p. 2040, 2020.

[12] H. An and S. J. Noh, "High-order averaging method of hydraulic conductivity for accurate soil moisture modeling," *Journal of Hydrology*, vol. 516, pp. 119–130, 2014.

[13] Y. Zeng, Z. Su, L. Wan, and J. Wen, "A simulation analysis of the advective effect on evaporation using a two-phase heat and mass flow model," *Water Resources Research*, vol. 47, no. 10, 2011.

[14] R. Duan, C. B. Fedler, and J. Borrelli, "Comparison of methods to estimate saturated hydraulic conductivity in Texas soils with grass," *Journal of Irrigation and Drainage Engineering*, vol. 138, no. 4, pp. 322–327, 2012.

[15] R. Gamie and F. De Smedt, "Experimental and statistical study of saturated hydraulic conductivity and relations with other soil properties of a desert soil," *European Journal of Soil Science*, vol. 69, no. 2, pp. 256–264, 2018.

[16] M. Rahmati, L. Weihermüller, J. Vanderborght et al., "Development and analysis of the soil water infiltration global database," *Earth System Science Data*, vol. 10, no. 3, pp. 1237–1263, 2018.

[17] A. Nemes, W. J. Rawls, and Y. A. Pachepsky, "Influence of organic matter on the estimation of saturated hydraulic conductivity," *Soil Science Society of America Journal*, vol. 69, no. 4, pp. 1330–1337, 2005.

[18] Y. Dai, W. Shangguan, Q. Duan, B. Liu, S. Fu, and G. Niu, "Development of a China dataset of soil hydraulic parameters using pedotransfer functions for land surface modeling," *Journal of Hydrometeorology*, vol. 14, no. 3, pp. 869–887, 2013.

[19] P. Shwetha and K. Varija, "Soil water retention curve from saturated hydraulic conductivity for sandy loam and loamy sand textured soils," *Aquatic Procedia*, vol. 4, pp. 1142–1149, 2015.

[20] M. V. Ottoni, T. B. Ottoni Filho, M. L. R. C. Lopes-Assad, and O. C. Rotunno Filho, "Pedotransfer functions for saturated hydraulic conductivity using a database with temperate and tropical climate soils," *Journal of Hydrology*, vol. 575, pp. 1345–1358, 2019.

[21] L. Weihermüller, P. Lehmann, M. Herbst et al., "Choice of pedotransfer functions matters when simulating soil water balance fluxes," *Journal of Advances in Modeling Earth Systems*, vol. 13, no. 3, Article ID e2020MS002404, 2021.

[22] R. K. Jaiswal, T. Thomas, R. V. Galkate, and J. Tyagi, "Soil water retention modeling using pedotransfer functions," *ISRN Civil Engineering*, vol. 2013, pp. 1–7, 2013.

[23] L. Xu, N. P. He, G. R. Yu, D. Wen, Y. Gao, and H. L. He, "Differences in pedotransfer functions of bulk density lead to high uncertainty in soil organic carbon estimation at regional scales: evidence from Chinese terrestrial ecosystems," *Journal of Geophysical Research: Biogeosciences*, vol. 120, no. 8, pp. 1567–1575, 2015.

[24] K. E. Saxton, W. J. Rawls, J. S. Romberger, and R. I. Papendick, "Estimating generalized soil-water characteristics from texture," *Soil Science Society of America Journal*, vol. 50, no. 4, 1986.

[25] H. Zhao, Y. Zeng, S. Lv, and Z. Su, "Analysis of soil hydraulic and thermal properties for land surface modeling over the Tibetan plateau," *Earth System Science Data*, vol. 10, no. 2, pp. 1031–1061, 2018.

[26] U. Dettmann, M. Bechtold, E. Frahm, and B. Tiemeyer, "On the applicability of unimodal and bimodal van genuchten–mualem based models to peat and other organic soils under evaporation conditions," *Journal of Hydrology*, vol. 515, pp. 103–115, 2014.

[27] D. Arisanty, J. Sartohadi, M. A. Marfai, and D. S. Hadmoko, "Sediment Dynamic in Barito Delta, Southern Kalimantan, Indonesia," in *Journal of Environments,* vol. 1, no. 1, pp. 30–37, 2014.

[28] P. Bassoullet, R. Djuwansah, D. Gouleau, and C. Marius, "Hydrosedimentological processes and soils of barito estuary (South Kalimantan, Indonesia)," *Oceanologica Acta*, vol. 9, pp. 217–226, 1986.

[29] N. J. Jarvis, L. Zavattaro, K. Rajkai et al., "Indirect estimation of near-saturated hydraulic conductivity from readily available soil information," *Geoderma*, vol. 108, no. 1-2, pp. 1–17, 2002.

[30] P. Nasta, J. A. Vrugt, and N. Romano, "Prediction of the saturated hydraulic conductivity from brooks and corey's water retention parameters," *Water Resources Research*, vol. 49, no. 5, pp. 2918–2925, 2013.

[31] S. A. Tomscha, S. Bentley, E. Platzer et al., "Multiple methods confirm wetland restoration improves ecosystem services," *Ecosystems and People*, vol. 17, no. 1, pp. 25–40, 2021.

[32] P. R. Knowles and P. A. Davies, "A method for the in-situ determination of the hydraulic conductivity of gravels as used in constructed wetlands for wastewater treatment," *Desalination and Water Treatment*, vol. 5, no. 1-3, pp. 257–266, 2009.

[33] J. Kruse, B. Lennartz, and P. Leinweber, "A modified method for measuring saturated hydraulic conductivity and anisotropy of fen peat samples," *Wetlands*, vol. 28, no. 2, pp. 527–531, 2008.

[34] R. A. MacMillan and P. A. Shary, "Chapter 9 landforms and landform elements in geomorphometry," *Developments in Soil Science*, vol. 33, pp. 227–254, 2009.

[35] USDA, "Module 3-usda textural soil classification," in *Soil Mechanics Level 1*USDA: United States of America, Washington, DC, USA, 1987.

[36] J. Moeys, *The Soil Texture Wizard: R Functions for Plotting, Classifying, Transforming and Exploring Soil Texture Data*, 2012.

[37] D. Arisanty, *Morphodynamic of Barito delta, Southern Kalimantan*, PhD Thesis, Gadjah Mada University, Yogyakarta, Indonesia, 2013.

[38] M. Weynants, H. Vereecken, and M. Javaux, "Revisiting vereecken pedotransfer functions: introducing a closed-form hydraulic model," *Vadose Zone Journal*, vol. 8, no. 1, pp. 86–95, 2009.

[39] T. Hengl, M. A. E. Miller, J. Križan et al., "African soil properties and nutrients mapped at 30 m spatial resolution using two-scale ensemble machine learning," *Scientific Reports*, vol. 11, no. 1, p. 6130, 2021.

[40] E. J. Pebesma, "Multivariable geostatistics in s: the gstat package," *Computers & Geosciences*, vol. 30, no. 7, pp. 683–691, 2004.

[41] P. J. Diggle and P. J. Ribeiro, "Bayesian inference," in *Model-based Geostatistics*Springer New York, New York, NY, USA, 2007.

[42] T. Hengl, *A Practical Guide to Geostatistical Mapping*, Office for Official Publications of the European Communities, Luxemburg, Europe, 2009.

[43] R. S. Bivand, E. Pebesma, and V. Gómez-Rubio, “Interpolation and geostatistics,” in *Applied Spatial Data Analysis with R*Springer, New York, NY, USA, 2013.

[44] J. J. Song, S. Kwon, and G. W. Lee, “Incorporation of parameter uncertainty into spatial interpolation using Bayesian trans-Gaussian kriging,” *Advances in Atmospheric Sciences*, vol. 32, no. 3, pp. 413–423, 2015.

[45] G. Ali, M. Sajjad, S. Kanwal et al., “Spatial–temporal characterization of rainfall in Pakistan during the past half-century (1961–2020),” *Scientific Reports*, vol. 11, no. 1, p. 6935, 2021.

[46] R. M. Lark, “Distinguishing spatially correlated random variation in soil from a ‘pure nugget’ process,” *Geoderma*, vol. 185-186, pp. 102–109, 2012.

[47] Y. He, K. L. Hu, Y. F. Huang, B. G. Li, and D. L. Chen, “Analysis of the anisotropic spatial variability and three-dimensional computer simulation of agricultural soil bulk density in an alluvial plain of north China,” *Mathematical and Computer Modelling*, vol. 51, no. 11-12, pp. 1351–1356, 2010.

[48] L. Tang and F. Hossain, “Transfer of satellite rainfall error from gaged to ungaged locations: how realistic will it be for the global precipitation mission?” *Geophysical Research Letters*, vol. 36, no. 10, Article ID L10405, 2009.

[49] L. Tang and F. Hossain, “Understanding the dynamics of transfer of satellite rainfall error metrics from gauged to ungauged satellite gridboxes using interpolation methods,” *Ieee Journal of Selected Topics in Applied Earth Observations and Remote Sensing*, vol. 4, pp. 844–856, 2011.

[50] N. Rahmawati, D. Arisanty, and D. Rosadi, *Supplementary Data for Paper: Soil Physical Characteristics and Saturated Hydraulic Conductivity in the Landform of Barito Delta, Kalimantan, indonesia*, 4TU.ResearchData, Delft, Netherlands, 2022.

[51] D. Wang, S. Zang, X. Wu et al., “Soil organic carbon stabilization in permafrost peatlands,” *Saudi Journal of Biological Sciences*, vol. 28, no. 12, pp. 7037–7045, 2021.

[52] D. Fan, C. Li, D. Wang, P. Wang, A. W. Archer, and S. F. Greb, “Morphology and sedimentation on open-coast intertidal flats of the Changjiang delta, China,” *Journal of Coastal Research*, pp. 23–35, 2004.

[53] D. Xu, R. Sun, T.-C. J. Yeh et al., “Mapping soil layers using electrical resistivity tomography and validation: sandbox experiments,” *Journal of Hydrology*, vol. 575, pp. 523–536, 2019.

[54] H. A. Illias, C. S. Su, and A. H. A. Bakar, “Investigation on soil resistivity of two-layer soil structures using finite element analysis method,” *IET Science, Measurement & Technology*, vol. 15, no. 2, pp. 120–129, 2021.

[55] P. E. Hehanussa, R. Djuwansyah, H. Haryono, and A. Dharma, *Sumberdaya Air Dan Tanah di Daerah Barito Kalimantan Selatan*, Indonesian Institute of Science (LIPI), Bandung, Indonesia, 1982.

[56] B. M. Vasantrao, P. J. Bhaskarrao, B. A. Mukund, G. R. Baburao, and P. S. Narayan, “Comparative study of wenner and schlumberger electrical resistivity method for groundwater investigation: a case study from dhule district (m.S.), India,” *Applied Water Science*, vol. 7, no. 8, pp. 4321–4340, 2017.

[57] H. M. Mohamad, B. Kasbi, M. Baba, Z. Adnan, S. Hardianshah, and S. Ismail, “Investigating peat soil stratigraphy and marine clay formation using the geophysical method in Padas valley, northern borneo,” *Applied and Environmental Soil Science*, vol. 2021, pp. 1–12, 2021.

[58] B. Peng, R. Feng, L. Wu, and Y. Shen, “Controlling conditions of the one-dimensional consolidation test on peat soil,” *Applied Sciences*, vol. 11, no. 23, p. 11125, 2021.

[59] J. Leifeld, M. Steffens, and A. Galego-Sala, “Sensitivity of peatland carbon loss to organic matter quality,” *Geophysical Research Letters*, vol. 39, no. 14, 2012.

[60] J. Leifeld, K. Klein, and C. Wüst-Galley, “Soil organic matter stoichiometry as indicator for peatland degradation,” *Scientific Reports*, vol. 10, no. 1, p. 7634, 2020.

[61] T. D. Moskal, L. Leskiw, M. A. Naeth, and D. S. Chanasyk, “Effect of organic carbon (peat) on moisture retention of peat: mineral mixes,” *Canadian Journal of Soil Science*, vol. 81, no. 2, pp. 205–211, 2001.

[62] P. K. Kolay and S. N. L. Taib, *Physical and Geotechnical Properties of Tropical Peat and its Stabilization*, B. Peat, Topcuoğlu and M. Turan, Eds., IntechOpen, London, UK, 2017.

[63] S. Kurnianto, J. Selker, J. Boone Kauffman, D. Murdiyarso, and J. T. Peterson, “The influence of land-cover changes on the variability of saturated hydraulic conductivity in tropical peatlands,” *Mitigation and Adaptation Strategies for Global Change*, vol. 24, no. 4, pp. 535–555, 2019.

[64] F. Rezanezhad, J. S. Price, W. L. Quinton, B. Lennartz, T. Milojevic, and P. Van Cappellen, “Structure of peat soils and implications for water storage, flow and solute transport: a review update for geochemists,” *Chemical Geology*, vol. 429, pp. 75–84, 2016.

[65] P. J. Morris, A. J. Baird, and L. R. Belyea, “Bridging the gap between models and measurements of peat hydraulic conductivity,” *Water Resources Research*, vol. 51, no. 7, pp. 5353–5364, 2015.